Atmos. Chem. Phys. Discuss., 13, 3451–3483, 2013
www.atmos-chem-phys-discuss.net/13/3451/2013/
doi:10.5194/acpd-13-3451-2013


Atmospheric Chemistry and Physics Discussions



# Relating aerosol absorption due to soot, organic carbon, and dust to emission sources determined from in-situ chemical measurements

**A. Cazorla[1,*], R. Bahadur[2], K. J. Suski[1], J. F. Cahill[1], D. Chand[3], B. Schmid[3], V. Ramanathan[2], and K. Prather[1,2]**

[1]Department of Chemistry and Biochemistry, University of California San Diego, La Jolla, California, USA
[2]Scripps Institution of Oceanography, University of California San Diego, La Jolla, California, USA
[3]Atmospheric Science and Global Change Division, Pacific Northwest National Laboratory, Richland, Washington, USA
[*]now at: Departamento de Física Aplicada, Universidad de Granada, Granada, Spain

Received: 15 December 2012 – Accepted: 22 January 2013 – Published: 6 February 2013

Correspondence to: K. Prather (kprather@ucsd.edu)

Published by Copernicus Publications on behalf of the European Geosciences Union.







## Abstract

Estimating the aerosol contribution to the global or regional radiative forcing can take advantage of the relationship between the spectral aerosol optical properties and the size and chemical composition of aerosol. Long term global optical measurements from observational networks or satellites can be used in such studies. Using in-situ chemical mixing state measurements can help us to constrain the limitations of such estimates.

In this study, the Absorption Ångström Exponent (AAE) and the Scattering Ångström Exponent (SAE) derived from 10 operational AERONET sites in California are combined for deducing chemical speciation based on wavelength dependence of the optical properties. In addition, in-situ optical properties and single particle chemical composition measured during three aircraft field campaigns in California between 2010 and 2011 are combined in order to validate the methodology used for the estimates of aerosol composition using spectral optical properties.

Results from this study indicate a dominance of mixed types in the classification leading to an underestimation of the primary sources, however secondary sources are better classified. The distinction between carbonaceous aerosols from fossil fuel and biomass burning origins is not clear, since their optical properties are similar. On the other hand, knowledge of the aerosol sources in California from chemical studies help to identify other misclassification such as the dust contribution.

## 1 Introduction

Atmospheric aerosol particles are one of the most variable components of the Earth's atmosphere, and affect the Earth's radiative balance and climate directly by absorbing and scattering solar radiation (Haywood and Shine, 1995; Forster et al., 2007), and indirectly by acting as cloud condensation nuclei, changing the microphysical properties of clouds (Kaufman et al., 2005; Forster et al., 2007).





ACPD
13, 3451–3483, 2013



Absorption of solar radiation due to aerosol particles is mainly caused by carbonaceous particles (elemental carbon, EC, and organic carbon, OC) and mineral dust. The absorbing fraction of carbonaceous aerosols has been estimated as the second largest contributor to global warming (Jacobson et al., 2000; Ramanathan and Carmichael, 2008). However, the absorbing properties are strongly dependent on the mixing state of the particles (Bond and Bergstrom 2006; Schnaiter et al., 2005). Further, current model estimates of aerosol forcing ascribe solar absorption entirely to elemental carbon (EC), treating the organic fraction (OC) as scattering (Koch et al., 2007; Myhre et al., 2008) and therefore may be underestimating the aerosol warming potential. Though this is a reasonable assumption in regions dominated by fossil fuel combustion, not only does carbon from all emission sources contain both elemental and organic fractions (Chow et al., 2009), but non-soot OC, particularly that emitted from biomass burning processes has a significant absorbing component at short wavelengths that may be comparable to the EC absorption (Jacobson, 1999; Kirchstetter et al., 2004; Andreae and Gelencser, 2006; Hoffer et al., 2006; Magi et al., 2009). A separation of the total aerosol absorption into different chemical species is therefore essential; both for constraining the large uncertainties in current aerosol forcing estimates (Forster et al., 2007) and for informing emissions based control policy. Detailed studies of the chemical composition and size distribution of aerosol particles, and how they relate to the optical properties is therefore essential to evaluate their impact on climate.

Russell at al. (2010) highlighted that many recent studies have shown the persistent connections between aerosol composition and the wavelength dependence of absorption. Thus, numerous studies have classified aerosol types from optical properties measured on ground stations (Eck et al., 1999; Dubovik et al., 2000; Collaud Coen et al., 2004; Fialho et al., 2005; Meloni et al., 2006; Kalapureddy et al., 2009; Mielonen et al., 2009) and from satellites (Higurashi and Nakajima, 2002; Barnaba and Gobbi, 2004; Jeong and Li, 2005; Kaufman et al., 2005; Torres et al., 2005; Kaskaoutis et al., 2007; Kim et al., 2007; Yu et al., 2009). In this study, in-situ optical properties and single particle chemical composition measured during three aircraft field campaigns are





ACPD
13, 3451–3483, 2013



combined in order to validate a methodology for the estimation of aerosol composition using spectral optical properties. In addition, this approach is extended and applied to a long term remote sensing optical measurements database, i.e. AERONET (Holben et al., 1998), using data from California stations and separating between northern and southern California and by seasons (winter/spring and summer/autumn). A total of 10 AERONET stations were analyzed using Level 2.0 aerosol inversion data (Table 1).

## 2 Methodology and results

### 2.1 Remote sensing measurements

Most previous studies showing a connection between aerosol types and optical properties were based on remote sensing measurements at locations with a strong dominant type or source, e.g. deserts, urban polluted areas, regions prone to wildfires, etc. Russell et al. (2010) used the Absorption Ångström Exponent (AAE) as an indicator of aerosol composition and they showed a clustering by aerosol types on an AAE vs. EAE (Extinction Ångström Exponent) scatter plot.

In this study, we apply a similar methodology, dividing the AAE vs. SAE (Scattering Ångström Exponent) space, the Ångström matrix, in different regions that are associated with different absorbing aerosol sources using AERONET measurements from 33 stations around the world with a dominant species. In order to calculate the AAE and SAE, the Single Scattering Albedo (SSA) derived by inversion in AERONET is used to calculate the Absorption and Scattering components of the AOD. Using Level 2.0 AERONET, only measurement with AOD at 440 nm greater than 0.4 are used for which the uncertainty of the AOD is between 0.01 and 0.02 depending on the wavelength (Holben et al., 1998), and this uncertainty results in a variation of 0.03 to 0.04 in the Ångstrom exponent (Schuster et al., 2006) and of 0.03 to 0.07 in the SSA (Dubovik et al., 2000). Then, AAE and SAE are calculated using Eq. (1) and Eq. (2), respectively:





ACPD
13, 3451–3483, 2013



$$\mathrm{AAE} = -\frac{\log\left(\frac{\mathrm{AAOD}(\lambda_1)}{\mathrm{AAOD}(\lambda_2)}\right)}{\log\left(\frac{\lambda_1}{\lambda_2}\right)} \quad (1)$$

$$\mathrm{SAE} = -\frac{\log\left(\frac{\mathrm{SAOD}(\lambda_1)}{\mathrm{SAOD}(\lambda_2)}\right)}{\log\left(\frac{\lambda_1}{\lambda_2}\right)} \quad (2)$$

where the wavelengths, $\lambda_1$ and $\lambda_2$, are 440 and 675 nm, respectively.

The spectral dependency of the absorption coefficient, AAE in Eq. (1), can be related to the source of absorbing aerosol. Black carbon typically follows a $\lambda^{-1}$ spectral dependency, yielding an AAE of 1 (Bergstrom et al., 2002), while organic carbon in biomass smoke aerosols and mineral dust contributed to light absorption in the ultraviolet and blue spectral regions yielding an AAE greater than 1 (Kirchstetter et al., 2004). On the other hand, the spectral dependency of the scattering coefficient, the SAE as shown in Eq. (2), depends primarily on the dominant size mode of the particles, ranging from 4 to 0 where larger numbers associate with small particles, i.e. fine mode, and smaller numbers suggest the dominance of large particles, i.e. coarse mode (Bergstrom et al., 2007).

Thus, in a very intuitive way, the AAE vs. SAE space partitions into regions that correlate to combinations of smaller and bigger particles and, particles that follow the $\lambda^{-1}$ trend for absorption, and those with absorption enhancement on the shorter wavelengths. The principal advantage of this dual size-chemistry related partitioning is that in the ideal case it separates the three aerosol absorbing species – EC, OC, and mineral dust. First, measurements representing dust separate along the SAE axis, as dust is primarily found in the coarse mode as compared to carbonaceous aerosols that are primarily in the fine and ultra-fine mode close to emission sources. Second, EC is an efficient absorber at all wavelengths compared to OC which absorbs strongly only at short wavelengths, separating these species along the AAE axis. In addition to these





ACPD
13, 3451–3483, 2013



ideal cases we can relate the remainder of the phase space to aerosols with predicted combinations of SAE (representing size) and AAE (representing chemistry), and their mixtures. Therefore, a comparison with in-situ chemical measurements, as presented in this work, is an invaluable aid in relating measured ambient aerosols as quantified by their size and chemistry to their optical properties. Figure 1 illustrates the division of the Ångström matrix with labels for the aerosol types based on the optical properties, and it shows data from the 33 AERONET stations color coded by dominant type. Table 2 lists the stations and its location and dominant aerosol species. Measurements from dust dominant stations fall mainly into the dust dominant area ("upper left quadrant"), however some measurements fall into the phase space representing polluted dust, mixed aerosols, or the coarse coated type. On the other hand, for ambient measurements, there is a larger overlap between fossil fuel and biomass burning related sources since all combustion produces both EC and OC, and there are no pure EC or OC ambient measurements. However, the fossil fuel category presents more variability in size than the biomass burning category due to the origin of the measurements. Whereas biomass burning dominant stations are mainly areas prone to wildfires, the stations marked as fossil fuel correspond to urban areas that are expected to contain a large amount of primary carbonaceous aerosols, but likely also contain larger aerosol particles (either lofted dust, or scattering aerosols such as sulfates), and likely also contain aged secondary aerosols due to high $NO_x$ and ozone conditions. Bahadur et al. (2012) provide further details on the full parameterization of the SAE-AAE phase space using a global set of aerosol measurements. Although the method of Bahadur et al. (2012) provides an effective mathematical scheme for attributing aerosol absorption between EC, OC, and dust, it does not provide insights into their emission sources in complex mixed environments.

To gain a better understanding of how the optical properties of aerosols relate to emissions, we use California as an initial test case, where the Ångström matrix can be compared to a large wealth of field data. We use measurements from a total of ten operational AERONET stations in California to obtain the spectral and optical properties





ACPD
13, 3451–3483, 2013



of the aerosols. The stations are divided by region, into Northern California for the stations with latitude above 36° N and Southern California for the stations below 36° N. Data are also divided by seasons grouping winter and spring in one season and summer and autumn in another season. Table 1 presents the name, location and available period of time in years for the 10 California AERONET stations and they are also shown on the map in Fig. 2. Applying the Ångström matrix, we obtain an estimate for the contribution of absorbers in California by means of optical properties. Figure 3 shows the contribution for the different regions and seasons in pie charts. Figure 3a shows the contribution for Northern California during winter/spring; Fig. 3b shows the contribution for Northern California during summer/autumn, Fig. 3c, d shows the contributions for Southern California during winter/spring and summer/autumn, respectively. Both seasons in northern California show similar aerosol contribution and they are dominated by a mixture of EC and OC aerosol that contribute over 40 % of all measurements. The difference lies in the coated large particles and mix types. For southern California, the summer/autumn season is dominated by a mixture, or EC and OC aerosol (almost 40 %) as well as OC and OC mixed with dust type. The winter/spring season is dominated by dust (over 45 %) and coated large particles (almost 30 %).

### 2.2 In-situ aircraft measurements

Using the in-situ optical properties and chemical composition measured during the three aircraft field campaigns, we can establish a link between the optical properties, in this case the AAE and the SAE, and the measured chemical composition of the aerosol particles.

In-situ data were measured during three aircraft field campaigns performed in California. CalNex 2010 was a joint field study coordinated by the California Air Resources Board (CARB), the National Oceanic and Atmospheric Administration (NOAA) and the California Energy Commission (CEC), with a primary goal to study atmospheric processes over California and the eastern Pacific coastal region. Measurements used in this work were taken on the Center for Interdisciplinary Remotely-Piloted Aircraft





ACPD
13, 3451–3483, 2013



Studies (CIRPAS) Twin Otter, flying mainly in the Los Angeles basin during May 2010. CARES (Carbonaceous Aerosols and Radiative Effects Study), was a field study funded but the US Department of Energy (DOE) Atmospheric Radiation Measurement (ARM) program, and was designed to increase scientific knowledge about evolution of black carbon and secondary organic aerosols from both urban/manmade and biogenic sources. Data used from this campaign were measured onboard the DOE Gulfstream-1 (G-1), based in Sacramento during June 2010. The CalWater 2011 field campaign, funded by CEC, was designed to better assess the effects aerosols have on precipitation in the Sierra Nevada during the winter season. Data used from this campaign were collected onboard the DOE G-1, based in Sacramento, between February and March 2011. Table 3 summarizes the name and location of the field campaigns, and the optical properties measured onboard used in this work. The different aircrafts contained instrumentation for the retrieval of the optical properties of aerosols, i.e. absorption and scattering coefficients. Figure 2 shows the flight paths for the three campaigns.

The absorption coefficient, $\sigma_a$ was derived using a Particle Soot Absorption Photometer (PSAP) at 462, 523 and 648 nm sampling from an iso-kinetic inlet. The Scattering coefficient, $\sigma_s$, was measured using a nephelometer at 450, 550 and 700 nm during CARES and CalWater, also sampling from an iso-kinetic inlet, and derived from a Passive Cavity Aerosol Spectrometer Probe (PCASP) size distribution, in the range of 0.1 to 3 µm, applying Mie theory (using a refractive index of 1.5) during CalNex. PSAP data were corrected based on Bond et al. (1999) and Ogren (2010) and nephelometer data were corrected based on Anderson and Ogren (1998). AAE and SAE were calculated applying Eqs. (1) and (2), respectively using $\sigma_a$ instead of the column integrate value (A-AOD) and $\sigma_s$ instead of the S-AOD. Wavelengths used as $\lambda_1$ and $\lambda_2$ were 462 and 648 nm for the PSAP and 450 and 700 for the nephelometer, since those are closer to the AERONET wavelength used in Sect. 2.1.

Measurements of the chemical composition of individual particles during the three aircraft campaigns were performed using the aircraft aerosol time-of-flight mass spectrometer (A-ATOFMS) (Pratt et al., 2009). The A-ATOFMS measures, in real time,





ACPD
13, 3451–3483, 2013



the size and chemical composition of individual particles ranging in size from 100 to 2500 nm during CalWater and from 80 to 1000 nm during CalNex and CARES. Following a $^{210}$Po neutralizer and pressure controlled inlet (Bahreini et al., 2003), particles are focused in an aerodynamic lens system. The particles are optically detected by two 532 nm lasers spaced 6.0 cm apart, providing particle velocity and, ultimately, vacuum aerodynamic diameter ($d_{va}$). Finally, species are desorbed and ionized using 266 nm radiation from a Q-switched Nd : YAG laser operating at ~ 0.4–1.0 mJ. Positive and negative ion mass spectra resulting from individual particles are measured in a dual-polarity time-of-flight mass spectrometer.

Spectra are grouped into chemically similar clusters using the ART-2- a algorithm (Song et al., 1999). The initial clusters are then manually grouped in a small set of clusters based on the identification of the mass spectral peaks that correspond to the most probable ions for a given mass-to-charge ratio (*m/z*) based on previous lab and field studies. These clusters are then classified into an absorbing source: primary fossil fuel, secondary fossil fuel, primary biomass burning, secondary biomass burning and dust, excluding other non-absorbing sources. Figure 4 shows a representative mass spectrum for each aerosol source.

Briefly, primary fossil fuel particles are characterized by the presence of carbon cluster ion peaks: $C_n^+$ and $C_n^-$, representative of the elemental carbon (EC), and spectra that also contain weak *m/z* 27 ($C_2H_3^+$), 37 ($C_3H^+$) and 39 ($C_3H_3^+$). Secondary fossil fuel particles contain *m/z* 27 ($C_2H_3^+$/$CHN^+$), 37 ($C_3H^+$), 39 ($C_3H_3^+$) and 43 ($C_2H_3O^+$) in the positive spectra and mainly nitrate and sulfate ion peaks in the negative ion mass spectra: *m/z* −62 ($NO_3^-$) and −97($HSO_4^-$), respectively (Silva and Prather, 2000; Spencer and Prather, 2006; Moffet and Prather, 2009). Biomass burning particles are characterized by an intense potassium peak *m/z* 39 ($K^+$) with less intense carbonaceous markers (e.g. *m/z* 12 ($C^+$), 27 ($C_2H_3^+$), 36 ($C_3^+$), 37 ($C_3H^+$)) (Silva et al., 1999; Hudson et al., 2004). The difference between primary and secondary biomass burning is established by looking at the negative spectra that presents carbon clusters in the case of primary biomass burning or mainly nitrate/sulfates in the case of secondary





ACPD
13, 3451–3483, 2013



biomass burning. Finally, dust is characterized by inorganic ion peaks, e.g. *m/z* 27 ($Al^+$), 39 ($K^+$), and/or 40 ($Ca^+$), and the presence of silicates: −60 ($SiO_2^-$) and −76 ($SiO_3^-$) (Silva et al., 2000).

A summary of the overall chemical composition detected during the three campaigns is shown in Fig. 5. Each pie chart represents the number fraction of absorbing sources detected during CalNex on the left panel, CARES in the middle, and CalWater on the right panel. Also each campaign, because of the location and dates, can be associated with a region and season. Therefore, CalNex corresponds with southern California during the summer, CARES is northern California also during the summer, and CalWater is northern California during the winter. Both seasons in northern California present similar sources with a contribution dominated by secondary fossil fuel aerosol and biomass burning. Also, more dust is detected during the winter. In southern California, the contribution from primary fossil fuel (35 %) and secondary fossil fuel (47 %) dominates in the summer.

## 2.3 Validation

In order to validate the Ångström matrix we matched the spectral optical properties and the chemical composition measured during the flights. For each flight, we calculated the 5-min average of the AAE and SAE. On the other hand, for the same 5-min periods, we calculated the fraction of the different chemical sources detected with the A-ATOFMS. We only considered periods with a dominant source, i.e. 75 % of the particles detected by the A-ATOFMS are from one source.

Thus, we screen the data using the 5-min average values that correspond with a dominant source. The AAE and SAE values that match the dominant source criteria are represented, in Fig. 6, on an AAE vs. SAE scatter plot with color representing the dominant source. Figure 6a–c corresponds to each different field campaign (CalNex, CARES and CALWATER, respectively). AAE is smaller on average during CalNex than during CARES, consistent with the type of dominant aerosol detected, mainly primary fossil fuel during CalNex, i.e. elemental carbon, in contrast with the secondary fossil





ACPD
13, 3451–3483, 2013



fuel particles that dominate during CARES. The number of samples from the CalWater campaign is small, as the flights focused on clouds and not many data samples were acquired from cloud free air. SAE shows less variability during CalNex than during CARES, but we need to take into account that the inlets were different during these campaigns, thus the range of particle sizes entering the inlet of the aircraft may vary. As discussed by Schmid et al. (2006) the Twin Otter samples aerosol from an iso-kinetic inlet whose passing efficiency was tested in airborne and wind tunnel experiments by Hegg et al. (2005). They found no appreciable loss in efficiency for particles smaller than 3.5 µm diameter at the Twin Otter sampling velocity of 50 $m\,s^{-1}$. For larger particles, the efficiency decreases rapidly but levels off at an efficiency of slightly better than 0.6 for particles 5.5–9 µm (the latter being the upper diameter of their characterization). The G-1 iso-kinet inlet used in CARES and CALWATER has not yet undergone the same testing. Manufacturer specifications call for passing efficiency near unity dropping to 50 % at 5 µm diameter at the G-1 research speed of 100 $m\,s^{-1}$. This claim has been substantiated with comparisons with ground-based nephelometers during fly-bys in CARES (Zaveri et al., 2012).

Since the AAE is related to the chemistry, Fig. 6d shows a frequency histogram of the AAE associated to the aerosol sources showing that primary fossil fuel particles have a mean value of AAE = 1.1 ± 0.6, which is close to the expected 1 for black carbon. Secondary fossil fuel particles can be associated with an AAE = 1.5 ± 0.3 and biomass burning to AAE = 1.8 ± 0.4.

Finally, we apply the Ångström matrix to the in-situ optical properties, obtaining an estimate of the aerosol composition using optical properties that can be compared with the actual chemical composition. Table 4 shows a contingency table where the rows are the chemical composition detected with the A-ATOFMS and columns are the different estimated aerosol types from the Ångström matrix. Values presented are percentages of measurements classified in one type or another and they sum 100 across rows. Primary fossil fuel sources, i.e. elemental carbon, were classified mainly as organic carbon or a mixture of organic carbon and elemental carbon or dust. Secondary fossil





ACPD
13, 3451–3483, 2013



fuel sources, i.e. secondary organic aerosols, fall mainly into the dust/EC mix (almost 40 %) indicating that those were particles with absorption properties similar to organic carbon, but larger in size. On the other hand, primary biomass burning sources were classified as organic carbon, organic mixed with dust, or well mix types. Secondary biomass burning sources are classified in almost 60 % into the organic carbon or organic carbon mixed with dust categories. Finally, dust sources were only significant during CalWater. However, the Ångström matrix does not classify them correctly as dust dominated type mainly because of the small amount of dust measurements.

## 3 Discussion

The estimates of aerosol types applying the Ångström matrix to the California AERONET stations (Fig. 3) show similar aerosol contributions in both seasons in northern California. Over 40 % of the contribution is due to a mixture of EC and OC, about 10 % due to EC, and 11 % due to OC or OC/dust mixture. For southern California, during the summer/autumn season almost 40 % of the aerosol contribution corresponds to a mixture of EC and OC, 27 % corresponds to OC or OC/dust types and 5 % corresponds to EC. The winter/spring season is dominated by dust (over 45 %) and coated large particles (almost 30 %) and no EC type is present.

The EC/OC mixture type seems to dominate in the Ångström matrix classification and indicates the difficulty of separating the sources from column integrated measurements. More fossil fuel sources (primary and secondary) were expected in southern California since it is a more populated, urban area, and the chemical composition detected during the aircraft campaigns for southern California (Fig. 5a) shows about 33 % of aerosol contribution due to primary fossil fuel sources, 47 % due to secondary fossil fuel sources, and about 15 % due to biomass burning sources. Figure 6d shows that the chemistry component of the Ångström matrix (the AAE) has a mean value of 1.1 for primary fossil fuel sources, 1.5 for secondary fossil fuel sources and 1.8 for biomass burning. All those sources would fall into the EC/OC mixture type or the OC type,





ACPD
13, 3451–3483, 2013



with some overlapping on the different sources, and leaving the EC type misclassified. On the other hand, northern California was expected to have more biomass burning sources respect to the south because of the less populated and more rural environment, and the aircraft data in northern California (Fig. 5b, c) indicates about 40 % of the contribution due to secondary fossil fuel sources and about 30 % due to biomass burning sources with a small contribution due to primary fossil fuel sources (about 7 to 10 %). Again, the overlapping of the optical properties results in the EC/OC mixture type dominating the classification.

Pure dust is not a significant source except for southern California during winter/spring. This is most likely a misclassification. The dust type measurements were concentrated in the UCLA and MISR-JPL AERONET stations, both in the Los Angeles metropolitan area, and dust is not expected to make such large contributions in urban areas. This suggests that those dust cases were instead larger hygroscopic organic carbon particles that had undergone aqueous phase processing. The aerosol species producing strong absorption at short wavelengths and primarily in the coarse mode are most likely humic-like substances (HULIS) species formed by fog or cloud processing. These aerosols have been detected in California in previous studies (e.g. Qin and Prather, 2006; Qin et al., 2012) and represent organic carbon particles, but are larger than 1 µm due to their water content, therefore they might have spectral properties similar to dust, i.e. they are large particles and absorb more radiation at shorter wavelengths (AAE > 1) which can fall in the Dust dominant or Dust/EC mixture types in the Ångström matrix. On the other hand, the in-situ chemical composition from the aircraft campaigns indicates the larger contribution due to dust from northern California during the winter as compare to the summer (14 % vs. 6 %). During the CalWater flights, dust particles were detected mainly at higher altitudes in layers, while during CARES flights were focused at much lower altitudes. Long range transported dust crossing the Pacific has been detected during the winter in northern California and it is thought to have an impact on the precipitation in California (Ault et al., 2011).





ACPD
13, 3451–3483, 2013



The differences in sources leading to absorption in the varying regions of California, as shown in Fig. 5, could be biased by the objectives of the flights during each of the campaigns. During CalNex, the flights were comprised of mainly low level passes within the boundary layer in the Los Angeles area, very close to the sources of pollution. On the other hand, CARES also had flights with passes over the Sierra foothills (away from urban sources in the Sacramento area), and intercepting plumes from fires if they were present. CalWater focused on clouds and most of the flights were either over the Sierra foothills or over the coastal area.

The overall in-situ spectral properties agree with the detected chemical composition. By looking at Fig. 6, we can see that the chemical component of the Ångström matrix, the AAE, is smaller on average during CalNex than during CARES, consistent with the type of dominant aerosol detected, more primary fossil fuel during CalNex, in contrast with the secondary fossil fuel and biomass that dominate during CARES. The number of samples for CalWater is small, as the flights focused on clouds. Also, Fig. 6d shows that the AAE has a mean value of $1.1 \pm 0.6$ for primary fossil fuel sources, secondary fossil fuel sources can be associated with an AAE $= 1.5 \pm 0.3$, and biomass burning to AAE $= 1.8 \pm 0.4$. These values agree with the values expected for BC (AAE $= 1$) and OC (AAE $> 1$). More dust data are needed to establish good statistics for this source. On the other hand, the size component of the Ångström matrix, the SAE, shows less variability during CalNex than during CARES, but we need to take into account that the cut size of the aircraft sampling inlets and the A-ATOFMS limits the sampling of the largest aerosol particles.

Finally, the application of the Ångström matrix to the in-situ aircraft measurements and comparison with the chemical composition of the aerosol (Table 4) shows some of the limitations of the Ångström matrix. Particles detected as a primary fossil fuel source, i.e. elemental carbon, were classified mainly as organic carbon or a mixture of organic carbon and elemental carbon or dust. This reinforces the conclusions extracted from the comparison of the overall chemistry composition for the different regions and seasons in California. The external mixing of aerosol on a column integrated value like the





ACPD
13, 3451–3483, 2013



AOD, or its absorption and scattering components, would yield to a higher AAE value and, therefore misclassifies the EC type (primary fossil fuel source). Particles detected as secondary fossil fuel, i.e. secondary organic aerosols, fall mainly into the dust/EC mix (almost 40 %) indicating that the those were particles with absorption properties similar to organic carbon (AAE > 1), but larger in size. This could be biased by the size detection limit of the sampling inlets onboard the aircrafts and the A-ATOFMS. Primary biomass burning measurements were limited: 5.7, 2.3 and 0.6 % of the overall particles detected in CalNex, CARES and CalWater, respectively (Fig. 5), but when detected as dominant, the Ångström matrix classified them as organic carbon or organic mixed with dust (50 %), or well mix types (the other 50 %). The amount of data from this source is very limited and more values are necessary for accurate statistics. Secondary biomass burning dominant sources are the ones that the Ångström matrix classifies the best, with almost 60 % falling into the organic carbon or organic carbon mixed with dust. Finally, the dust source is only significant during CalWater (14 % of total) and more data is necessary for accurate statistics.

## 4 Conclusions

Numerous studies have estimated aerosol composition from spectral optical measurements using ground remote sensing measurements, e.g. AERONET or satellites. These networks or satellite platforms provide optical properties on a global scale, which are needed for the assessment of the contribution of aerosols to the radiative forcing and climate. Including information on the chemical composition of aerosols from discrete cases, specifically the absorbing particles sources, can help to identify the sources that contribute to the forcing globally.

In this study, we present a methodology for the estimation of chemical composition from spectral optical measurements, and explored its limitations using in-situ optical measurements and chemical composition. Our estimates are based on the division of the Absorption Ångström Exponent vs. Scattering Ångström Exponent space and it





ACPD
13, 3451–3483, 2013



is applied to ten AERONET stations in California. In order to validate this approach, in-situ optical properties from three aircraft campaigns that took place in California between 2010 and 2011 with single particle chemical composition measurements were analyzed. To explore the range of sources, the AERONET data and in-situ aircraft data were divided into regions (northern and southern California) and seasons (winter/spring and summer/autumn).

In-situ chemical composition results reveal a higher contribution from fossil fuel sources in southern California in contrast with more biomass burning sources in northern California. This agrees with the in-situ spectral optical measurements and other studies (e.g. Cahill et al., 2012). The estimation of aerosol types with spectral optical properties shows a dominance of mixed types. Pure EC is underestimated since it is being classified as a mixture of EC and OC. This is expected from column integrated aerosol optical properties, and the overlapping of sources and optical properties is also revealed in the in-situ measurements. Comparison of detailed chemical measurements and spectral properties reveals that secondary organic aerosols processed in aqueous phase might be a significant contributor in urban areas with a predominance of smog events, such as the Los Angeles basin.

On the other hand, applying the technique to estimate the chemical composition with spectral optical measurements, the Ångström matrix, to in-situ optical measurements including the actual chemical composition also show the limitations in the optical separation of the sources. Primary sources are difficult to classify, since the column integrated measurements result in particles being classified as a mixture. Secondary species are well classified, but the separation between fossil fuel and biomass burning sources has limitations because of the overlapping of the optical properties. In general, OC is better identified as a biomass burning source than a secondary fossil fuel source. Despite these limitations, the detailed comparison reveals the significance of aerosol absorption due OC, which is currently underestimated in climate models, in addition to EC. A significant number of absorption events are related to brown carbon from both





ACPD
13, 3451–3483, 2013



biomass and secondary sources indicating that it must be a primary consideration while developing future climate mitigation policies.

In conclusion, the availability of long-term global optical properties provides an opportunity for longer term estimates of aerosol types over a more larger spatial scale. However co-located studies for some overlapping period of time with actual chemical composition measurements are necessary in order to constrain the applicability of the technique to specific regions. This will be necessary if we want to develop this tool into a general approach for accurately addressing the contribution of different aerosol sources to regional and global radiative forcing.

*Acknowledgements.* Funding for this work was provided by CARB under agreement no. 08-323. The statements and conclusions in this report are those of the researchers and not necessarily those of the California Air Resources Board. The mention of any commercial products, their source, or their use in connection with the material reported is not construed as actual or implied endorsement of such products.

We would like to thank the field staff involved in the deployment of the G1 during CARES and CalWater. The deployment of the G-1 was funded by the Atmospheric Radiation Measurement (ARM) Program sponsored by the US Department of Energy (DOE), Office of Biological and Environmental Research (OBER) and the US DOE's Atmospheric System Research (ASR) Program under Contract DE-AC06-76RLO 1830 at PNNL for CARES, and by the California Energy Commission under contract CEC 500-09-043 and 500-09-032 for CalWater. The deployment of the Twin Otter during CalNex was supported by NOAA grant NA090AR4310128. We also would like to thank the people involved during the CalNex campaign, and especially to Haflidi Jonsson who provided useful insight with the optical measurement from the Twin Otter.

## References

Anderson, T. L. and Ogren, J. A.: Determining aerosol radiative properties using the TSI-3563 integrating nephelometer, Aerosol Sci. Techn., 29, 57–69, 1998.

Andreae, M. O. and Gelencsér, A.: Black carbon or brown carbon? The nature of light-absorbing carbonaceous aerosols, Atmos. Chem. Phys., 6, 3131–3148, doi:10.5194/acp-6-3131-2006, 2006.





ACPD

13, 3451–3483, 2013



Ault, A. P., Williams, C. R., White, A. B., Neiman, P. J., Creamean, J. M., Gaston, C. J., Ralph, F. M., and Prather, K. A. Detection of Asian dust in California orographic precipitation, J. Geophys. Res., 116, 1–15, 2011.
Bahadur, R., Praveen, P. S., Xu, Y. Y., and Ramanathan, V.: Solar absorption by elemental carbon and brown carbon determined from spectral observations, P. Natl. Acad. Sci. USA, 109, 17366–17371, 2012.
Bahreini, R., Jimenez, J. L., Wang, J., Flagan, R. C., Seinfeld, J. H., Jayne, J. T., and Worsnop, D. R.: Aircraft-based aerosol size and composition measurements during ACE-Asia using an Aerodyne aerosol mass spectrometer, J. Geophys. Res., 108, 8645, doi:10.1029/2002JD003226, 2003.
Barnaba, F. and Gobbi, G. P.: Aerosol seasonal variability over the Mediterranean region and relative impact of maritime, continental and Saharan dust particles over the basin from MODIS data in the year 2001, Atmos. Chem. Phys., 4, 2367–2391, doi:10.5194/acp-4-2367-2004, 2004.
Bergstrom, R. W., Russell, P. B., and Hignett, P.: Wavelength dependence of the absorption of black carbon particles: predictions and results from the TARFOX experiment and implications for the aerosol single scattering albedo, J. Atmos. Sci., 59, 567–577, 2002.
Bergstrom, R. W., Pilewskie, P., Russell, P. B., Redemann, J., Bond, T. C., Quinn, P. K., and Sierau, B.: Spectral absorption properties of atmospheric aerosols, Atmos. Chem. Phys., 7, 5937-5943, doi:10.5194/acp-7-5937-2007, 2007.
Bond, T. C. and Bergstrom, R. W.: Light absorption by carbonaceous particles: an investigative review, Aerosol. Sci. Techn., 40, 27–67, 2006.
Bond, T. C., Anderson, T. L., and Campbell, D.: Calibration and intercomparison of filter-based measurements of visible light absorption by aerosols, Aerosol Sci. Techn., 30, 582–600, 1999.
Cahill, J. F., Suski, K., Seinfeld, J. H., Zaveri, R. A., and Prather, K. A.: The mixing state of carbonaceous aerosol particles in northern and southern California measured during CARES and CalNex 2010, Atmos. Chem. Phys., 12, 10989–11002, doi:10.5194/acp-12-10989-2012, 2012.
Chow, J. C., Watson, J. G., Doraiswamy, P., Chen, L. W. A., Sodeman, D. A., Lowenthal, D. H., Park, K., Arnott, W. P., and Motallebi, N.: Aerosol light absorption, black carbon, and elemental carbon at the Fresno Supersite, California, Atmos. Res., 93, 874–887, 2009.





ACPD
13, 3451–3483, 2013



Collaud Coen, M., Weingartner, E., Schaub, D., Hueglin, C., Corrigan, C., Henning, S., Schwikowski, M., and Baltensperger, U.: Saharan dust events at the Jungfraujoch: detection by wavelength dependence of the single scattering albedo and first climatology analysis, Atmos. Chem. Phys., 4, 2465–2480, doi:10.5194/acp-4-2465-2004, 2004.

Dubovik, O. and King, M. D.: A flexible inversion algorithm for retrieval of aerosol optical properties from Sun and sky radiance measurements, J. Geophys. Res., 105, 20673–20696, 2000.

Dubovik, O., Holben, B. N., Eck, T. F., Smirnov, A., Kaufman, Y. J., King, M. D., Tanré, D., and Slutsker, I.: Variability of absorption and optical properties of key aerosol types observed in worldwide locations, J. Atmos. Sci., 59, 590–608, 2002.

Eck, T. F., Holben, B. N., Reid, J. S., Dubovik, O., Smirnov, A., O'Neill, N. T., Slutsker, I., and Kinne, S.: Wavelength dependence of the optical depth of biomass burning, urban, and desert dust aerosols, J. Geophys. Res., 104, 31333–31349, 1999.

Fialho, P., Hansen, A. D. A., and Honrath, R. E.: Absorption coefficients by aerosols in remote areas: a new approach to decouple dust and black carbon absorption coefficients using sevenwavelength Aethalometer data, J. Aerosol Sci., 36, 267–282, 2005.

Forster, P., Ramaswamy, V., Artaxo, P., Berntsen, T., Betts, R., Fahey, D. W., Haywood, J., Lean, J., Lowe, D. C., Myhre, G., Nganga, J., Prinn, R., Raga, G., Schulz, M., and Van Dorland, R.: Changes in atmospheric constituents and in radiative forcing, in: Climate Change 2007: The Physical Science Basis, Contribution of Working Group I to the Fourth Assessment Report of the Intergovernmental Panel on Climate Change, edited by: Solomon, S., Qin, D., Manning, M., Chen, Z., Marquis, M., Averyt, K. B., Tignor, M., and Miller, H. L., Cambridge University Press, Cambridge, UK and New York, NY, USA, 2007.

Haywood, J. M. and Shine, K. P.: The effect of anthropogenic sulfate and soot aerosol on the clear sky planetary radiation budget, Geophys. Res. Lett., 22, 603–606, 1995.

Hegg, D. A., Covert, D. S., Jonsson, H., and Covert, P. A.: Determination of the transmission efficiency of an aircraft aerosol inlet, Aerosol Sci. Techn., 39, 966–971, 2005.

Higurashi, A. and Nakajima, T.: Detection of aerosol types over the East China Sea near Japan from four-channel satellite data, Geophys. Res. Lett., 29, 1836, doi:10.1029/2002GL015357, 2002.

Hoffer, A., Gelencsér, A., Guyon, P., Kiss, G., Schmid, O., Frank, G. P., Artaxo, P., and Andreae, M. O.: Optical properties of humic-like substances (HULIS) in biomass-burning aerosols, Atmos. Chem. Phys., 6, 3563–3570, doi:10.5194/acp-6-3563-2006, 2006.





ACPD
13, 3451–3483, 2013



Holben, B. N., Eck, T. F., Slutsker, I., Tanré, D., Buis, J. P., Setzer, A., Vermote, E., Reagan, J. A., Kaufman, Y. J., Nakajima, T., Lavenu, F., Jankowiak, I., and Smirnov, A.: AERONET – a federated instrument network and data archive for aerosol characterization, Remote Sens. Environ., 66, 1–16, 1998.

Hudson, P. K., Murphy, D. M., Cziczo, D. J., Thomson, D. S., de Gouw, J. A., Warneke, C., Holloway, J., Jost, J. R., and Hubler, G.: Biomass-burning particle measurements: characteristic composition and chemical processing, J. Geophys. Res., 109, D23S27, doi:10.1029/2003JD004398, 2004.

Jacobson, M. Z.: Isolating nitrated and aromatic aerosols and nitrated aromatic gases as sources of ultraviolet light absorption, J. Gephys. Res., 104, 3527–3542, 1999.

Jacobson, M. C., Hansson, H. C., Noone, K. J., and Charlson, R. J.: Organic atmospheric aerosols: review and state of the science, Rev. Geophys., 38, 267–294, 2000.

Jeong, M. J. and Li, Z.: Quality, compatibility, and synergy analyses of global aerosol products derived from the advanced very high resolution radiometer and total ozone mapping spectrometer, J. Geophys. Res., 110, D10S08, doi:10.1029/2004JD004647, 2005.

Kalapureddy, M. C. R., Kaskaoutis, D. G., Ernest Raj, P., Devara, P. C. S., Kambezidis, H. D., Kosmopoulos, P. G., and Nastos, P. T.: Identification of aerosol type over the Arabian Sea in the premonsoon season during the Integrated Campaign for Aerosols, Gases and Radiation Budget (ICARB), J. Geophys. Res., 114, D17203, doi:10.1029/2009JD011826, 2009.

Kaskaoutis, D. G., Kosmopoulos, P., Kambezidis, H. D., and Nastos, P. T.: Aerosol climatology and discrimination of different types over Athens, Greece based on MODIS data, Atmos. Environ., 41, 7315–7329, 2007.

Kaufman, Y. J., Boucher, O., Tanré, D., Chin, M., Remer, L. A., and Takemura, T.: Aerosol anthropogenic component estimated from satellite data, Geophys. Res. Lett., 32, L17804, doi:10.1029/2005GL023125, 2005.

Kim, J., Lee, J., Lee, H. C., Higurashi, A., Takemura, T., and Song, C. H.: Consistency of the aerosol type classification from satellite remote sensing during the atmospheric brown cloud-East Asia regional experiment campaign, J. Geophys. Res., 112, D22S33, doi:10.1029/2006JD008201, 2007.

Kirchstetter, T. W., Novakov, T., and Hobbs, P. V.: Evidence that the spectral dependence of light absorption by aerosols is affected by organic carbon, J. Goephys. Res., 109, D21208, 1–12, 2004.





ACPD
13, 3451–3483, 2013



Koch, D., Bond, T. C., Streets, D., Unger, N., and van der Werf, G. R.: Global impacts of aerosols from particular source regions and sectors, J. Geophys. Res., 112, D02205, doi:10.1029/2005JD007024, 2007.

Magi, B. I., Ginoux, P., Ming, Y., and Ramaswamy, V.: Evaluation of tropical and extratropical Southern Hemisphere African aerosol properties simulated by a climate model, J. Geophys. Res., 114, D14204, doi:10.1029/2008JD011128, 2009.

Meloni, D., di Sarra, A., Pace, G., and Monteleone, F.: Aerosol optical properties at Lampedusa (Central Mediterranean). 2. Determination of single scattering albedo at two wavelengths for different aerosol types, Atmos. Chem. Phys., 6, 715–727, doi:10.5194/acp-6-715-2006, 2006.

Mielonen, T., Arola, A., Komppula, M., Kukkonen, J., Koskinen, J., de Leeuw, G., and Lehtinen, K. E. J.: Comparison of CALIOP level 2 aerosol subtypes to aerosol types derived from AERONET inversion data, Geophys. Res. Lett., 36, L18804, doi:10.1029/2009GL039609, 2009.

Moffet, R. C. and Prather, K. A.: In situ measurements of the mixing state and optical properties of soot: implications for radiative forcing estimates, P. Natl. Acad. Sci. USA, 106, 11872–11877, 2009.

Myhre, G., Hoyle, C. R., Berglen, T. F., Johnson, B. T., and Haywood, J. M.: Modeling of the solar radiative impact of biomass burning aerosols during the Dust and Biomass-burning Experiment (DABEX), J. Geophys. Res. 113, D00C16, doi:10.1029/2008JD009857, 2008.

Ogren, J. A.: Comment on "Calibration and intercomparison of filter-based measurements of visible light absorption by aerosols", Aerosol Sci. Techn., 44, 589–591, 2010.

Pratt, K. A., Mayer, J. E., Holecek, J. C., Moffet, R. C., Sanchez, R. O., Rebotier, T. P., Furutani, H., Gonin, M., Fuhrer, K., Su, Y., Guazzotti, S., and Prather, K.: Development and characterization of an aircraft aerosol time-of-flight mass spectrometer, Anal. Chem., 81, 1792–1800, 2009.

Qin, X. and Prather, K.: Impact of biomass emissions on particle chemistry during the california regional particulate air quality study, Int. J. Mass Spectrom., 258, 142–150, 2006.

Qin, X., Pratt, K. A., Shields, L. G., Toner, S. M., and Prather, K. A.: Seasonal comparisons of single-particle chemical mixing state in Riverside, CA, Atmos. Environ., 59, 587–596, 2012.

Ramanathan, V. and Carmichael, G.: Global and regional climate changes due to black carbon, Nat. Geosci., 1, 221–227, 2008.





ACPD
13, 3451–3483, 2013



Russell, P. B., Bergstrom, R. W., Shinozuka, Y., Clarke, A. D., DeCarlo, P. F., Jimenez, J. L., Livingston, J. M., Redemann, J., Dubovik, O., and Strawa, A.: Absorption Angstrom Exponent in AERONET and related data as an indicator of aerosol composition, Atmos. Chem. Phys., 10, 1155–1169, doi:10.5194/acp-10-1155-2010, 2010.

Schmid B., Ferrare, R., Flynn, C., Elleman, R., Covert, D., Strawa, A., Welton, E., Turner, D., Jonsson, H., Redemann, J., Eilers, J., Ricci, K., Hallar, A. G., Clayton, M., Michalsky, J., Smirnov, A., Holben, B., and Barnard. J.: How well do state-of-the-art techniques measuring the vertical profile of tropospheric aerosol extinction compare?, J. Geophys. Res., 111, D05S07, doi:10.1029/2005JD005837, 2006.

Schnaiter, M., Linke, C., Mohler, O., Naumann, K. H., Saathoff, H., Wagner, R., Schurath, U., and Wehner, B.: Absorption amplification of black carbon internally mixed with secondary organic aerosol, J. Geophys. Res.-Atmos., 110, D19204, doi:10.1029/2005JD006046, 2005.

Schuster, G. L., Dubovik, O., and Holben, B. N.: Ångstrom exponent and bimodal aerosol size distributions, J. Geophys. Res., 111, D07207, doi:10.1029/2005JD006328, 2006.

Silva, P. J. and Prather, K. A.: Interpretation of mass spectra from organic compounds in aerosol time-of-flight mass spectrometry, Anal. Chem., 72, 3553–3562, 2000.

Silva, P. J., Liu, D. Y., Noble, C. A., and Prather, K. A.: Size and chemical characterization of individual particles resulting from biomass burning of local Southern California species, Environ. Sci. Technol., 33, 3068–3076, 1999.

Silva, P. J., Carlin, R. A., and Prather, K. A.: Single particle analysis of suspended soil dust from Southern California, Atmos. Environ., 34, 1811–1820, 2000.

Song, X. H., Hopke, P. K., Fergenson, D. P., and Prather, K. A.: Classification of single particles analyzed by ATOFMS using an artificial neural network, ART-2A, Anal. Chem., 71, 860–865, 1999.

Spencer, M. T. and Prather, K. A.: Using ATOFMS to determine OC/EC mass fractions in particles, Aerosol Sci. Technol., 40, 585–594, 2006

Torres, O., Bhartia, P. K., Syniuk, A., and Welton, E.: TOMS measurements of aerosol absorption from space: comparison to SAFARI 2000 ground based observations, J. Geophys. Res., 110, D10S18, doi:10.1029/2004JD004611, 2005.

Yu, H., Chin, M., Remer, L. A., Kleidman, R. G., Bellouin, N., Bian, H., and Diehl, T.: Variability of marine aerosol fine-mode fraction and estimates of anthropogenic aerosol component over cloud-free oceans from the Moderate Resolution Imaging Spectroradiometer (MODIS), J. Geophys. Res., 114, D10206, doi:10.1029/2008JD010648, 2009.





ACPD
13, 3451–3483, 2013



Zaveri, R. A., Shaw, W. J., Cziczo, D. J., Schmid, B., Ferrare, R. A., Alexander, M. L., Alexandrov, M., Alvarez, R. J., Arnott, W. P., Atkinson, D. B., Baidar, S., Banta, R. M., Barnard, J. C., Beranek, J., Berg, L. K., Brechtel, F., Brewer, W. A., Cahill, J. F., Cairns, B., Cappa, C. D., Chand, D., China, S., Comstock, J. M., Dubey, M. K., Easter, R. C., Erickson, M. H., Fast, J. D., Floerchinger, C., Flowers, B. A., Fortner, E., Gaffney, J. S., Gilles, M. K., Gorkowski, K., Gustafson, W. I., Gyawali, M., Hair, J., Hardesty, R. M., Harworth, J. W., Herndon, S., Hiranuma, N., Hostetler, C., Hubbe, J. M., Jayne, J. T., Jeong, H., Jobson, B. T., Kassianov, E. I., Kleinman, L. I., Kluzek, C., Knighton, B., Kolesar, K. R., Kuang, C., Kubátová, A., Langford, A. O., Laskin, A., Laulainen, N., Marchbanks, R. D., Mazzoleni, C., Mei, F., Moffet, R. C., Nelson, D., Obland, M. D., Oetjen, H., Onasch, T. B., Ortega, I., Ottaviani, M., Pekour, M., Prather, K. A., Radney, J. G., Rogers, R. R., Sandberg, S. P., Sedlacek, A., Senff, C. J., Senum, G., Setyan, A., Shilling, J. E., Shrivastava, M., Song, C., Springston, S. R., Subramanian, R., Suski, K., Tomlinson, J., Volkamer, R., Wallace, H. W., Wang, J., Weickmann, A. M., Worsnop, D. R., Yu, X.-Y., Zelenyuk, A., and Zhang, Q.: Overview of the 2010 Carbonaceous Aerosols and Radiative Effects Study (CARES), Atmos. Chem. Phys., 12, 7647–7687, doi:10.5194/acp-12-7647-2012, 2012.





ACPD
13, 3451–3483, 2013



**Table 1.** Location and data availability of the AERONET stations in California.

| AERONET station | Latitude (° N) | Longitude (° W) | Data Availability |
|---|---|---|---|
| Fresno | 36.782 | 119.773 | 2002–2011 |
| La Jolla | 32.870 | 117.250 | 1994–2011 |
| MISR-JPL | 34.119 | 118.174 | 1996–2009 |
| Monterey | 36.593 | 121.855 | 1998–2011 |
| Moss Landing | 36.793 | 121.788 | 2004–2006 |
| San Nicolas | 33.257 | 119.487 | 1997–2007 |
| Table Mountain | 34.380 | 117.680 | 1998–2011 |
| Trinidad Head | 41.054 | 124.151 | 2005–2011 |
| UCLA | 34.070 | 118.450 | 2000–2009 |
| UCSB | 34.415 | 119.845 | 1994–2011 |





ACPD
13, 3451–3483, 2013



**Table 2.** List of the AERONET stations around the world with dominant sources used for the creation of the Ångström matrix.

| AERONET station | Latitude (° N) | Longitude (° W) | Main source |
|---|---|---|---|
| Billerica | 42.53 | 71.27 | Fossil Fuel |
| CCNY | 40.82 | 73.95 | Fossil Fuel |
| Dayton | 39.77 | 84.11 | Fossil Fuel |
| Fresno | 36.78 | 119.77 | Fossil Fuel |
| GSFC | 38.99 | 76.84 | Fossil Fuel |
| Halifax | 44.64 | 63.59 | Fossil Fuel |
| Hamburg | 53.57 | −9.97 | Fossil Fuel |
| Hong Kong | 22.21 | −114.26 | Fossil Fuel |
| IFT Leipzig | 51.35 | −12.43 | Fossil Fuel |
| Mainz | 49.99 | −8.3 | Fossil Fuel |
| Maryland Sci. Cen. | 39.28 | 76.62 | Fossil Fuel |
| New Delhi | 28.63 | −77.17 | Fossil Fuel |
| Palaiseau | 48.7 | −2.21 | Fossil Fuel |
| Philadelphia | 40.04 | 75 | Fossil Fuel |
| Rome Tor Vergata | 41.84 | −12.65 | Fossil Fuel |
| Sandy Hook | 40.45 | 73.99 | Fossil Fuel |
| UCLA | 34.07 | 118.45 | Fossil Fuel |
| Abracos Hill | 10.76 | 62.35 | Biomass Burning |
| Alta Floresta | −9.87 | 56.1 | Biomass Burning |
| Belterra | −2.65 | 54.95 | Biomass Burning |
| Campo Grande | −20.45 | 54.62 | Biomass Burning |
| CELAP-BA | −34.57 | 58.5 | Biomass Burning |
| Cordoba CETT | −31.52 | 64.46 | Biomass Burning |
| CUIABA Miranda | −15.73 | 56.02 | Biomass Burning |
| Mongu | −15.25 | −23.15 | Biomass Burning |
| Petrolina SONDA | −9.38 | 40.5 | Biomass Burning |
| Rio Branco | −9.96 | 67.87 | Biomass Burning |
| Skukuza Aeroport | −24.97 | −31.59 | Biomass Burning |
| Eilat | 29.5 | −34.92 | Dust |
| Hamim | 22.97 | −54.3 | Dust |
| Solar Village | 24.91 | −46.39 | Dust |
| Tamanrasset INM | 22.79 | −5.53 | Dust |
| Tamanrasset TMP | 22.79 | −5.53 | Dust |





ACPD
13, 3451–3483, 2013



**Table 3.** Name and location of the aircraft field campaigns and optical properties measured used in this work.

| Campaign Name | Location | Dates | Absorption Coefficient | Scattering Coefficient | Chemical composition |
|---|---|---|---|---|---|
| CalNex | Los Angeles basin | May 2010 | PSAP | PCASP size distribution | A-ATOFMS |
| CARES | Sacramento area and central valley | Jun 2010 | PSAP | Nephelometer | A-ATOFMS |
| CalWater | Sacramento area and central valley | Feb–Mar 2011 | PSAP | Nephelometer | A-ATOFMS |





ACPD
13, 3451–3483, 2013



**Table 4.** Contingency matrix constructed from the aircraft measurements representing the percentage of aerosol sources from the A-ATOMFS classified into the different Ångström matrix classes.

| | | Ångström Matrix | | | | | | | |
|---|---|---|---|---|---|---|---|---|---|
| | | EC dom. | EC/OC mix | OC dom. | OC/Dust mix | Dust dom. | Dust/EC mix | Coated | Mix |
| A-ATOFMS | Prim. Fossil Fuel | 1.20 | 27.71 | 31.33 | 21.69 | 1.20 | 0 | 10.84 | 6.02 |
| | Sec. Fossil Fuel | 0 | 0 | 10.47 | 27.91 | 8.14 | 39.53 | 9.30 | 4.65 |
| | Prim. Biomass | 0 | 0 | 25 | 25 | 0 | 0 | 0 | 50 |
| | Sec. Biomass | 0 | 3.70 | 18.52 | 40.74 | 14.81 | 0 | 18.52 | 3.70 |
| | Dust | 14.29 | 7.14 | 28.57 | 7.14 | 7.14 | 0 | 14.29 | 21.43 |





ACPD
13, 3451–3483, 2013



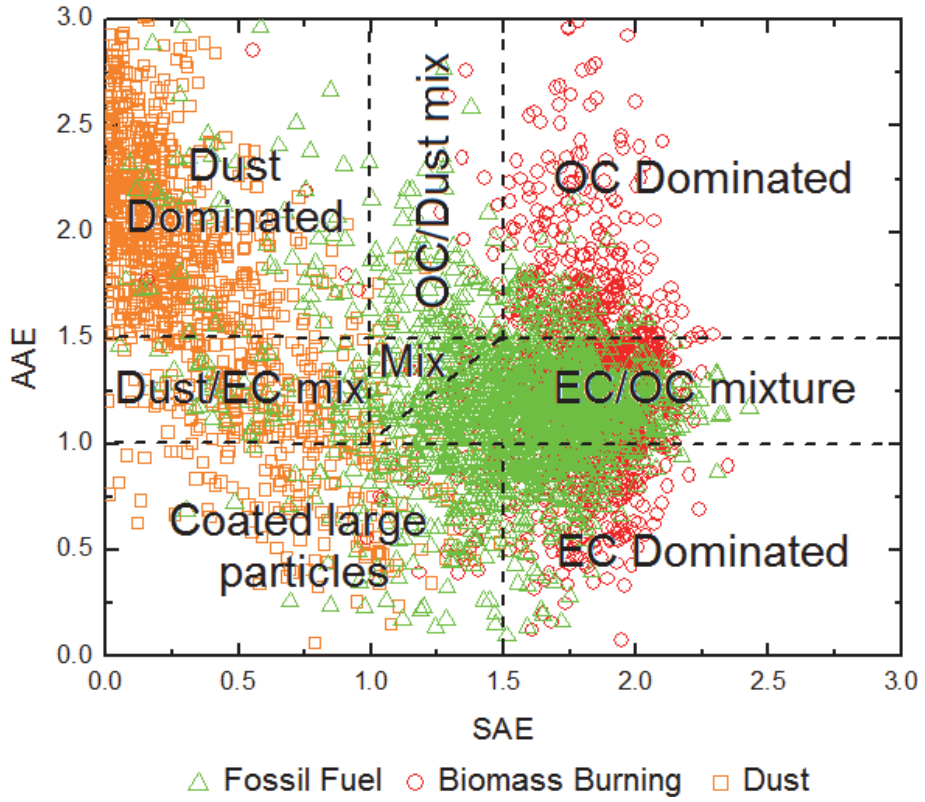


**Fig. 1.** Division of the Absorption Ångström Exponent vs. Scattering Ångström Exponent space, the Ångström matrix, overlapped with the AERONET measurements from stations with a dominant sources (fossil fuel, biomass burning or dust).





ACPD
13, 3451–3483, 2013



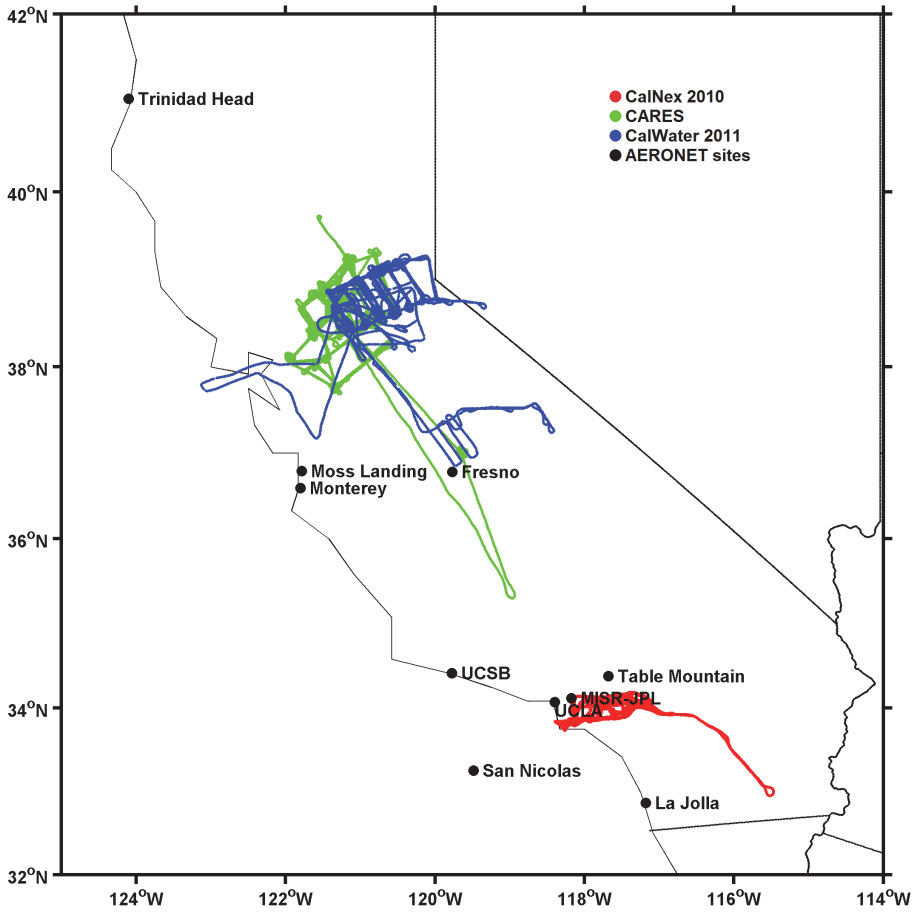


**Fig. 2.** Map of California with the flight paths of the aircraft campaigns and the location of the AERONET stations.





ACPD
13, 3451–3483, 2013



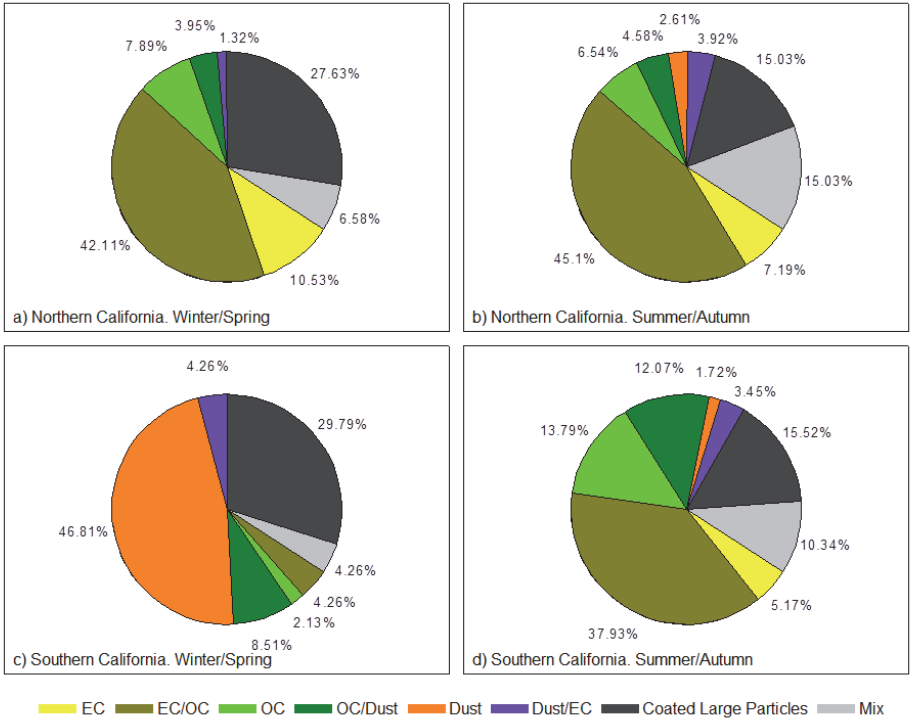


**Fig. 3.** Estimated chemical composition derived from AERONET stations in California separated by region and season: **(a)** Northern California – winter/spring, **(b)** Northern California – summer/autumn, **(c)** Southern California – winter/spring, and **(d)** Southern California – summer/autumn.





ACPD
13, 3451–3483, 2013



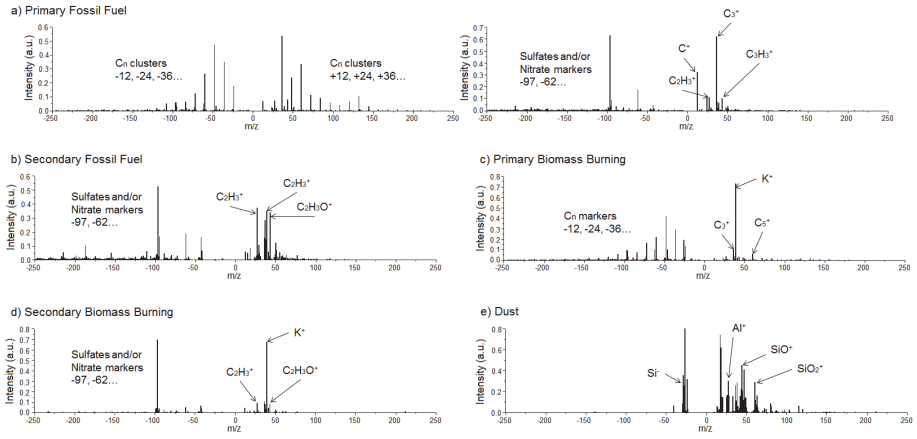


**Fig. 4.** Representative A-ATOFMS spectra for different aerosol sources **(a)** primary fossil fuel, **(b)** secondary fossil fuel, **(c)** primary biomass burning, **(d)** secondary biomass burning, and **(e)** dust.





ACPD
13, 3451–3483, 2013



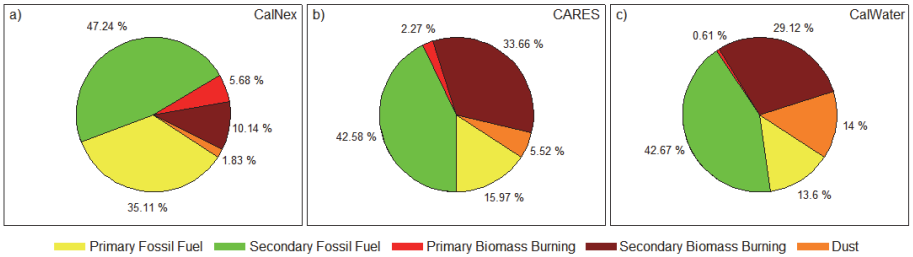


**Fig. 5.** Overall chemical composition detected with the A-ATOFMS in the three aircraft campaigns: **(a)** CalNex, **(b)** CARES, and **(c)** CalWater.





ACPD
13, 3451–3483, 2013



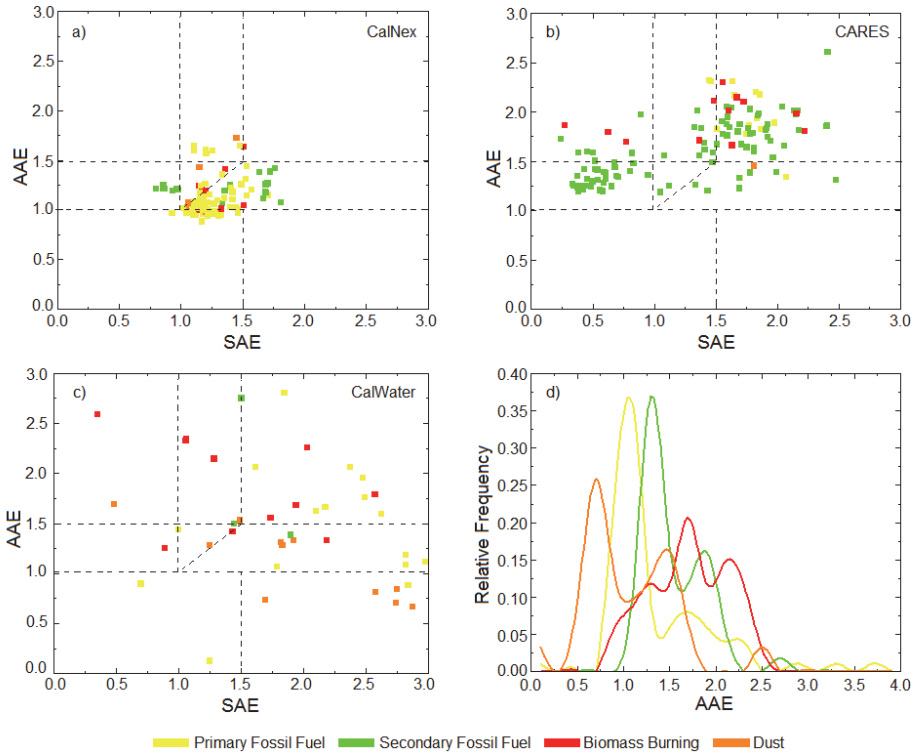


**Fig. 6.** Absorption Ångström Exponent vs. Scattering Ångström Exponent scatter plot of in-situ aircraft measurements for **(a)** CalNex, **(b)** CARES, and **(c)** CalWater where the color code represents the dominant aerosol source detected with the A-ATOFMS for each measurement. **(d)** is a frequency histogram of the Absorption Ångström Exponent for each aerosol source.





ACPD
13, 3451–3483, 2013